Generation of femtosecond laser pulses tunable from 380 nm to 465 nm via cascaded nonlinear optical mixing in a noncollinear optical parametric amplifier with a type-I phase matched BBO crystal

Chao-Kuei Lee, Jing-Yuan Zhang[+], J. Y. Huang and Ci-Ling Pan

Photon-Factory, Institute of Electro-Optical Engineering
National Chiao Tung University, Hsinchu, 30010 Taiwan, ROC
[+] *Department of Physics, Georgia Southern University, Statesboro, GA 30460, USA. Corresponding author*
chuckcklee@yahoo.com, *jyzhang@gasou.edu*

Abstract: We report the generation of tunable femtosecond pulses from 380nm to 465nm near the degenerate point of a 405-nm pumped type-I BBO noncollinearly phase-matched optical parametric amplifier (NOPA). The tunable UV/blue radiation is obtained from sum frequency generation (SFG) between the OPA output and the residual fundamental beam at 810-nm and cascaded second harmonic generation (SHG) of OPA. With a fixed seeding angle, the generated SFG and SHG covers from 385 nm to 465-nm. With a pumping energy of 75 μJ at 405 nm, the optical conversion efficiency from the pump to the tunable SFG is more than 5% and the efficiency of SHG of the OPA is about 2%.

OCIS codes: (190.4410) Nonlinear optical parametric processes; (190.7110) Ultrafast nonlinear optics; (190.4970) Parametric oscillators and amplifiers

References and links

1. A. H. Zewail, "Femtochemistry: Atomic-Scale Dynamics of the Chemical Bond," J. Phys. Chem. A **104**, 5660-5694 (2000).
2. N. H. Damrauer, G. Cerullo, A. Yeh, T. R. Boussie, C. V. Shank, J. K. McCusker, "Femtosecond Dynamics of Excited-State Evolution in $[Ru(bpy)_3]^{2+}$," Science **275**, 54-57 (1997).
3. T. Elsaesser, S. Mukamel, M. Murnane, N. F. Scherer, Ultrafast Phenomena **XII**, in: Proceedings of the 12th International Conference, Springer, New York, 2000.
4. W. Joosen , H. J. Bakker , L. D. Noordman , H. G. Muller , and H. B. van Linden, van den Heuvell, "Parametric generation in -barium borate of intense femtosecond pulses near 800 nm," J. Opt. Soc. Am. B **8**, 2087-2093 (1991).
5. P. Di Trapani , A. Andreoni , P. Foggi , C. Solcia , R. Danielius , and A. Piskarskas , "Efficient conversion of femtosecond blue pulses by traveling-wave parametric generation in non-collinear phase matching," Opt. Commun. **119**, 327-332 (1995).
6. T. Wilhelm, J. Piel, and E. Riedle, "Sub-20-fs pulses tunable across the visible from a blue-pumped single-pass noncollinear parametric converter," Opt. Lett. **22**, 1494-1496 (1997).
7. Jing-yuan Zhang, Aparna Prasad Shreenath, Mark Kimmel, Erik Zeek and Rick Trebino, and Stephan Link, "Measurement of the intensity and phase of attojoule femtosecond light pulses using optical parametric amplification cross-correlation frequency-resolved optical gating," Opt. Express **11**, 601-609 (2003), http://www.opticsexpress.org/abstract.cfm?URI=OPEX-11-6-601
8. Jing-yuan Zhang, Chao-Kuei Lee, J. Y. Huang, and Ci-Ling Pan, "Single-shot XFROG measurements of ultraweak femtosecond light pulses using beam-crossing optical-parametric-amplification," (submitted to Opt. Lett. 2003)

1. Introduction

Recent rapid progress in femtosecond laser technology has made it a powerful tool in the fields of ultrafast spectroscopy and material diagnostics [1-3]. By combining ultrashort intense pulses from amplified solid-state lasers with nonlinear optical techniques, one can generate widely tunable femtosecond light pulses from the near UV through the IR [4-6]. Among those developments, noncollinear optical parametric amplification (NOPA) seeded with white-light super continuum (WLS) had been widely employed. The use of a seeding pulse reduces the pumping threshold needed for optical parametric generation, and improves the pulse-to-pulse stability and spatial mode quality. NOPA also yields some unique advantages for reducing the group velocity mismatch (GVM), increasing the interaction length between the pump pulse and the seeder and therefore improving the parametric gain. However, owing to the limit of phase-matching condition, the tuning range for a 400-nm pumped type-I BBO-NOPA only covers from 460-nm to 720-nm in the signal branch and from 900-nm to 2.4 μm in the idler. A tuning gap exists from ~720-nm to ~900-nm, where the output energy of NOPA is significantly lower than that at other wavelengths. This is caused by the very broad bandwidth and low gain around the degenerate point. When the seeding angle is increased, the short wavelength-end of the tuning curve red shifts, which further narrows the tuning range. It is difficult to obtain tunable femtosecond pulses with wavelength shorter than 460-nm from a 400-nm-pumped BBO-OPA. This is unfortunate since tunable femtosecond pulses in the blue and the near UV region (<460 nm) are most useful in many applications ranging from investigations of wide band-gap materials to biomolecules. Various nonlinear optical wave-mixing processes, including sum frequency generation (SFG) and second harmonic generation (SHG), had been employed to convert the output of NOPA to short wavelength. However, the addition of SHG (or SFG) stage complicates femtosecond pulse profile and increase the difficulty of operation. Furthermore, the optical conversion efficiency of an external SHG stage for the OPA output is generally low due to serious walk-off, GVM and limited intensity.

In this paper we report the generation of tunable femtosecond pulses in the blue and near-UV region from 380-nm to 465-nm with a 405-nm pumped type I BBO-NOPA without any additional frequency-doubling crystal. The tunable radiation is attributed to cascaded second harmonic generation (SHG) of the generated OPA and sum frequency generation (SFG) process from the generated OPA and the residual pump laser beam at 810-nm from the while-light super continuum (WLS). With the configuration used, SFG can readily be generated in the OPA stage. By using a pump energy of 75 μJ at 405-nm, the tunable SFG from 380-nm and 465-nm has an output energy of 4 μJ. The output of SFG can be further improved by increasing the energy of either the pump at 405-nm or the residual beam at 810-nm. The output of SHG of the OPA is 1.5 μJ and it is tunable from 410-nm to 660-nm. The pulse durations of the SFG and SHG are about the same as that of the pump.

2. Experimental

2.1. Experimental arrangement

The schematic of our experimental setup is shown in Fig. 1. The output of a regeneratively amplified Ti: sapphire laser provides an output energy of more than 1 mJ per pulse at 810-nm with pulse duration of ~90 fs. The output of the laser is split into two parts by a 3-mm thick beam splitter: 5% of the beam reflected from the beam splitter is used to generate white-light supercontinuum (WLS) from a 2-mm CaF_2 plate with appropriate attenuation and focusing. The remaining energy transmitted through the beam-splitter passes through an adjustable attenuator, a 1:3 telescope and a delay-line before it is frequency-doubled to 405-nm with a 0.30-mm BBO. The SHG beam with energy adjustable between 50-120 μJ is used to pump the NOPA. The CaF_2 plate generates WLS with smaller chirp and the beam-splitter used may cause pulse broadening of the pump beam through GVD. Therefore the seeding pulse could be shorter than the pump of WLS (@810nm) to increase the seeding intensity and the output stability of the OPA can be significantly improved. The generated WLS is collimated by a parabolic mirror, and then is temporally and spatially overlapped with the pump beam in a 2-mm-long type-I BBO cut at $\theta=29^o$. The beam crossing angle α between the seeder and the pump of OPA (@405nm) is adjustable from 2 to 18 degrees. When the BBO is tuned to around the degenerate point of the OPA, its output becomes relatively weak and two bright, high-quality beams tunable in the near-UV and the deep blue region can be observed together with the optical parametric superfluorescence ring. The image shown in Fig. 1 is the spatial mode pattern of the system. The green ring is the parametric superfluorescence and the black spot in the middle of the ring indicates the position of the residual pump beam at 810 nm. To avoid saturating the CCD camera with the residual pump beam of OPA at 405-nm, we punched a hole on the observation screen to let most of the residual pump beam go through the hole. As shown in Fig. 1, the red spot near the ring and on the right of the pump is the output of OPA. The bright spot on the left of the ring is the tunable SHG and the bright spot between the parametric superfluorescence ring and the pump of OPA (@405nm) is the SFG component.

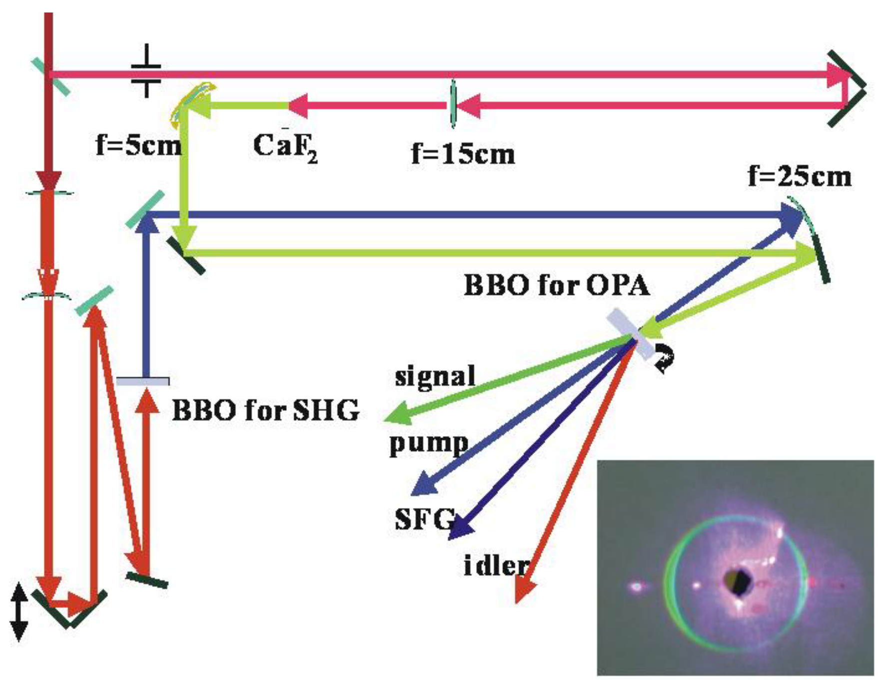

Fig. 1 Experimental setup of the OPA-SHG/SFG. The bright spot on the left of the parametric superfluorescence ring is the SHG component and the central spot is a pinhole to let the residual pump beam go through to avoid saturating the CCD camera. The spot between the pump of OPA and the SHG is the SFG component. The image is taken with a seeding angle of 8-degree.

2.2 Relation between the pumping intensity and the SFG/SHG output

With a seeding angle from 3 to 18 degrees, we discovered two bright spot. One can be attributed to the sum frequency generation (SFG) between the OPA component and the residual pump beam at 810-nm from WLS generation. The other, which is attributed to the second harmonic generation (SHG) from the idler of the OPA, is generated with the BBO crystal tuned to near the degenerate point. The wavelength of the SHG component can be changed from the near-UV, to the blue, the green or even to the red region. In the meantime, when the wavelength of the OPA approaches the degenerate point, a second spot, which is due to sum frequency generation (SFG) of the OPA output and the residual pump beam at 810 nm, can be seen. The 810-nm radiation was used for generating white-light supercontinuum (WLS). The pumping threshold for generating SHG and SFG components depends on the seeding angle: At a large seeding angle (~15^o), the SFG can be observed even below the pumping threshold of parametric superfluorescence. When the seeding angle is decreased to 6-8 degrees, in order to see the SFG/SHG spots with naked eye, the BBO crystal has to be pumped up to a level that the bright parametric fluorescence can be generated. At an even smaller seeding angle of 2-3 degrees, the SHG/SFG components are difficult to generate and the output is weaker. This can be understood as in the following: At a large seeding angle, the central wavelength of SFG is at around 410-nm and the central wavelength of SHG of the OPA is at 439nm, where the GVM of OPA is relatively small. This leads to a longer pulse walk-off distance and therefore the cascaded SFG/SHG is expected to yield a stronger output.

2.3 Tuning range of cascaded SFG and SHG

One can calculate the tuning range of SFG and SHG as a function of seeding angles and as a function of the orientation of the BBO crystal by taking into account the phase-matching conditions of NOPA and SFG/SHG and the group velocity mismatch (GVM) among the spectral components involved. We also found that the central wavelength of the SFG is adjustable from 410 and 440-nm with the seeding angle, while the tuning range of SHG covers a broader spectral range from 380 nm to 660 nm. The central wavelength of SFG/SHG becomes shorter at large seeding angle and longer at small seeding angle. When the seeding angle is fixed, the SFG/SHG can also be tuned by rotating the crystal. With a small seeding angle, the SFG is centered at 450-nm with the tuning range splitting into two parts. For this case, where GVM is large and the pulse walk-off distance becomes shorter, a higher pumping intensity is needed to generate the cascaded SFG and SHG.

The central wavelength and tuning range of the SFG/SHG beams are measured at the following three seeding angles: 14, 8, and 2 degrees. At 14 degree, the tuning range of SFG covers from 380-nm to 432-nm with a central wavelength at about 410-nm. It agrees very well with the prediction of theory. At a seeding angle of 8^o, the tuning range extends from 395 nm to 460 nm with a central wavelength shifted to 440-nm. At a seeding angle of 3 degrees, SFG is barely observable at 410 nm. The tuning range of SHG is generally broader than that of SFG.

It is known that at a large seeding angle, such as between 8 and 16 degree, favors SFG and SHG because the GVM between the OPA and the residual radiation at 810-nm is smaller. As the seeding angle becomes smaller, the SFG/SHG is weaker from the increased GVM between the OPA and the SFG. The effect of GVM is particularly important for a very short pumping laser pulse. The central wavelength of SFG/SHG can be controlled by the seeding angle, while the fine tuning of SFG/SHG can be done by rotating the angle of the BBO crystal.

Figure 2 shows the tuning characteristics of the generated SFG and SHG, respectively, at a seeding angle of 8-degree. The SFG is tuned by rotating the BBO crystal. A tuning range from 389 nm to 425-nm had been observed as shown in the top figure. The maximum output of SFG is at 400-nm. With the same seeding angle of 8 degree, the tuning range of the cascaded SHG of OPA covers a very broad spectral range from 410-nm to 660-nm. The maximum output occurs at 439-nm. The bottom figure shows the spectra of the tunable SHG at various angles of the BBO.

#2582 - $15.00 US Received June 06, 2003; Revised July 08, 2003

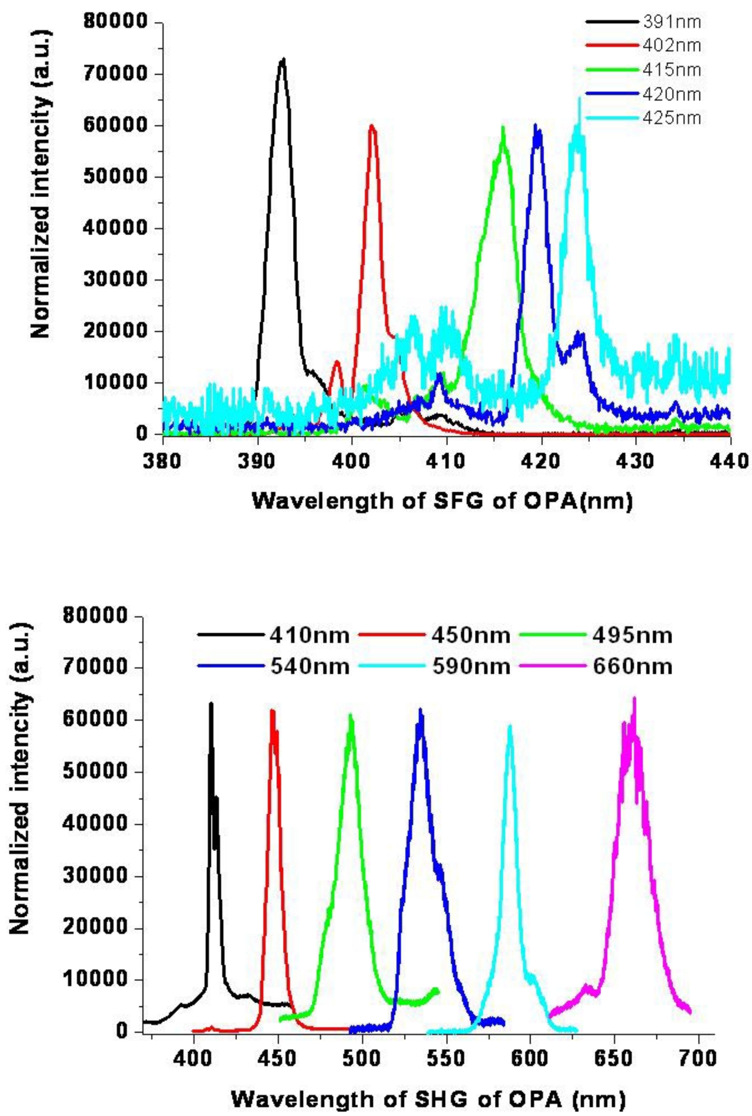

Fig. 2 Spectra of cascaded SFG (up-figure) and SHG (bottom-figure) of NOPA at various BBO orientations. The spectra were taken at a seeding angle of 8 degree.

It is seen from Fig. 2 that the tuning range of the cascaded SFG/SHG fills the gap of the tuning range of a 400-nm pumped OPA in the wavelength range shorter than 460-nm.

Experimentally, it is observed that the SFG and SHG can be generated simultaneously over a broad tuning range of the OPA. In order to understand such a phenomenon, a theoretical calculation was done to find the phase-matching conditions for the OPA, the cascaded SFG and SHG. It can be shown that when the seeding angle lies between 3 to 18 degrees, the phase-matching angle of the cascaded SFG and SHG of OPA is coincidently overlapped with that of a 400-nm pumped type-I BBO NOPA at its degenerate point. Figure 3 shows the relationship between the wavelengths of OPA, SFG and SHG and the angle of the

#2582 - $15.00 US
Received June 06, 2003; Revised July 08, 2003

BBO crystal at various seeding angles α. Clearly, the curves of SFG and SHG cross each other when the wavelength of OPA ranges from 0.7 to around 1.0 μm, indicating the coexistence of SFG and SHG in that wavelength range of the OPA. This explains why one can observe both SFG and SHG components simultaneously when the BBO crystal is tuned to around the degenerate point at 810 nm. The calculation in Fig. 3 agrees well with the experimental observation.

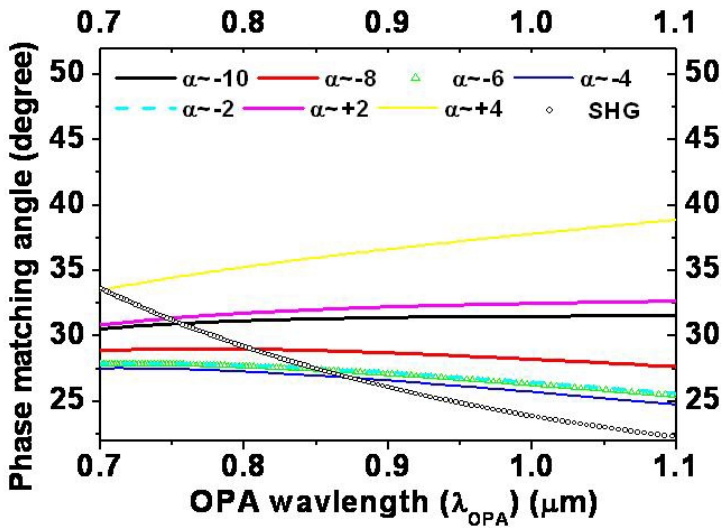

Fig. 3. Theoretical calculation on the relationship of phase-matching angle of SFG and SHG as a function of wavelength of OPA indicating the coexistence of SFG and SHG near the degenerate point of OPA at 810 nm.

2.4 Conversion efficiency of cascaded SFG-OPA

It is interesting to note that the cascaded SFG-OPA also exhibits fairly high optical conversion efficiency. With a pumping energy of 75-μJ/pulse at 405 nm, the total energy conversion efficiency from the pump to the OPA at signal wavelength around 580 nm is more than 25%, including 14 μJ in the signal branch and 5 μJ in the idler branch. With the same pumping energy and a residual seed energy of ~30 μJ at 810-nm, the output energy of SFG is 4.1 μJ, which corresponds to an energy conversion efficiency of more than 5%. The output energy of SHG is more than 1.5 μJ, yielding an energy conversion efficiency of about 2%. A simple way to further increase the SFG output is to excite it with higher pulse energy at 810-nm.

We note that one can produce tunable near UV-VIS femtosecond radiation by frequency-doubling the output of the OPA. However, this scheme requires a second BBO crystal for SHG and synchronous rotation of two crystals. This makes the wavelength tuning more complicated. Secondly, the surface loss at the second crystal would reduce the optical conversion efficiency when the second stage is used. Finally, when a second stage is used, the SHG needs to be done in a collinear way and large GVM is encountered. The SHG conversion efficiency of sub 100-fs laser pulses is mainly limited by the GVM and the pumping intensity. Therefore, the cascaded SFG is more efficient than SHG, no matter it is done internally or externally.

#2582 - $15.00 US
Received June 06, 2003; Revised July 08, 2003

2.5. Pulse shape of SFG

Using a newly developed OPA-based frequency-resolved optical gating (OPA-FROG) technique [7], we have analyzed the output of the NOPA to deduce the complex field profiles. Our measured and retrieved OPA-FROG traces show that there is no significant chirping in the output of OPA and the pulse duration of the OPA is about 75-fs. We can also measure the FROG-trace of the SFG and SHG outputs with a beam-crossing single-shot OPA/single-shot FROG technique [8], which allows measurements of femtosecond pulses in a single-shot fashion without mechanical scan of optical delay. It was found that the pulse width of the generated SFG is longer than that of the corresponding OPA and shorter than that of the 810-nm pump pulse. This confirms that the SFG pulse is a temporal convolution of the OPA component and the residual fundamental beam. The same measurements were also done with SHG output and it is found to be shorter than that of OPA.

3. Summary

In conclusion, we have successfully demonstrated, for the first time to our knowledge, the generation of femtosecond tunable pulse in the near-UV/visible via cascaded SFG-OPA or SHG with a single crystal. The device is pumped at 400 nm and operates near the degenerate point of a type-I non-collinearly phase-matched OPA. The energy conversion efficiency of the SFG is more than 5%, while that of SHG of OPA is about 2%. Our design provides a simple while effective way to extend the tuning range of a 400-nm pumped type-I BBO-OPA down to 380-nm without an additional frequency up-conversion stage. The beam quality and pulse shape of the SFG is found to be about the same as that of OPA output.

Acknowledgments

The authors acknowledge the sponsorship of National Science Council under various grants and the Pursuit of academic excellence program of the Ministry of Education, Republic of China. Dr. Jing-Yuan Zhang thanks the support of Georgia Southern University during his sabbatical leave.